LCAO MO Investigations on Lignin Model Compounds
VI. CNDO/CI Calculations of Electronic Spectra of Cinnamaldehyde Structures

Milan Remko and Jan Polčin

Pulp and Paper Research Institute, 890 20 Bratislava, Czechoslovakia

(Z. Naturforsch. **32a**, 59–65 [1977]; received August 9, 1977)

The electronic absorption spectra of cinnamaldehyde, o-, m-, p-hydroxycinnamaldehyde and 3-methoxy-4-hydroxy cinnamaldehyde were theoretically and experimentally studied, by means of the semiempirical CNDO/CI method. The calculated and observed transition energies were in good agreement.

Introduction

In the foregoing investigations[1,2], the electronic spectra of lignin model compounds of hydroxybenzaldehyde and quinoidic type were investigated by the CNDO/CI[3] method. In this study lignin model compounds of the cinnamaldehyde type (cinnamaldehyde, o-, m-, p-hydroxycinnamaldehyde, 3-methoxy-4-hydroxy cinnamaldehyde) have been theoretically and experimentally investigated. Cinnamaldehyde structures are suggested as very important chromogens of lignin[4]. Due to their absorption in the visible range of the spectrum they have to be destroyed during bleaching of lignified fibrous materials[5–7]. Thus the systematic experimental and theoretical study of these compounds in the ground and excited state is very important regarding the mentioned problems of lignin chemistry.

Experimental

The unsubstituted cinnamaldehyde used for the spectrophotometric measurements was a commercial preparation supplied by Loba-Chemie, Wien, freshly distilled before use. The o-, m-, p-hydroxycinnamaldehydes and the 3-methoxy-4-hydroxy cinnamaldehyde were synthetized according to procedures published in the literature[8].

The spectra were measured with the Perkin Elmer, Model 323 recording spectrophotometer. As the substances investigated showed a low solubility in nonpolar solvents, spectrally pure ethanol (95%) was used. The experimental spectra are shown on Figures 1 and 2.

Reprint requests to Dr. M. Remko and Dr. J. Polčin, Pulp and Paper Research Institute, *890 20 Bratislava*, Czechoslovakia.

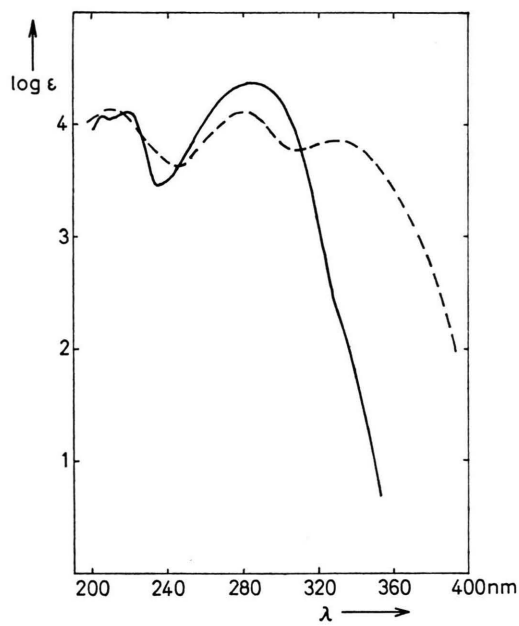

Fig. 1. Absorption spectra of cinnamaldehydes in ethanol;
———: cinnamaldehyde,
– – – –: o-hydroxycinnamaldehyde.

Calculations

For the calculation of the electronic structures and the electronic spectra of the molecules investigated, the CNDO method was applied in the modification of Del Bene and Jaffé[3]. The calculation of two-centre repulsion integrals was carried out by the Mataga-Nishimoto approximation[9]. In the configuration interaction twenty of the lowest monoexcited configurations were taken into account in all cases.

The parametrization of Kuehnlenz and Jaffé[10] was applied, using the experimental geometry from the study[11]. All the models were assumed to be

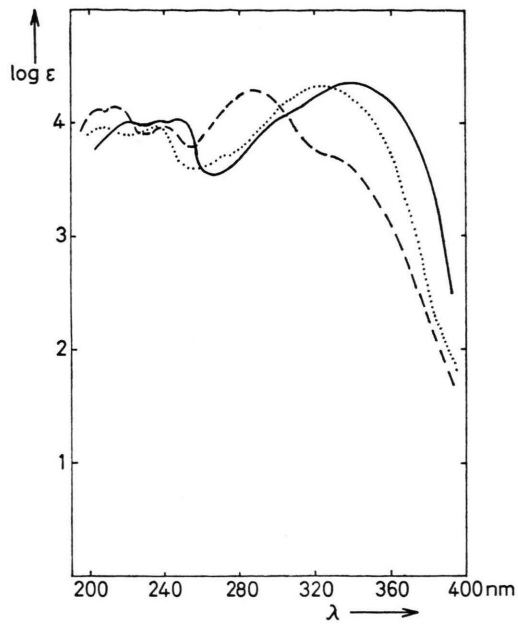

Fig. 2. Absorption spectra of cinnamaldehydes in ethanol;
———: 3-methoxy-4-hydroxy cinnamaldehyde,
– – – –: m-hydroxycinnamaldehyde,
.....: p-hydroxycinnamaldehyde.

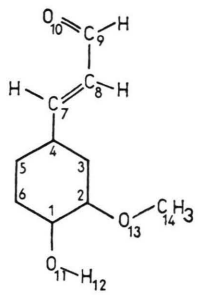

Fig. 3. Structure and numbering of atoms in cinnamaldehydes.

planar with C_s symmetry. The calculations were carried out with trans-cis isomers (Fig. 3) using the QCPE programme N. 174 on the Siemens 4004/150 computer in the Computing Center of the Komenský University, Bratislava.

Results and Discussion

1. Electronic States and Molecular Orbitals

The experimental and by the CNDO/CI method calculated energies and oscilator strengths are listed in Table 1. The calculated transition energies are in a good agreement with the experimental ones. All

Table 1. Singlet-singlet transitions in cinnamaldehydes.

Transition	Energy[a]		f	
	Obsd	Calcd	Obsd	Calcd
		Cinnamaldehyde		
A″	29.4	29.0		0
A′	35.1	36.8	0.524	0.0002
A′	40.0	37.6	0.080	0.425
A′	44.8	48.4	0.004	0.210
A″		49.0		0
A′	46.1	49.1	0.241	0.052
A″		51.9		0
A′	48.7	52.8	0.129	0.188
		m-Hydroxycinnamaldehyde		
A″	27.7	28.4		0
A′	30.9	35.1	0.142	0.043
A′	35.0	37.6	0.443	0.356
A′	42.0	46.7	0.203	0.318
A′	46.9	47.6	0.399	0.061
A″		48.7		0
A′	49.2	51.4	0.172	0.136
		o-Hydroxycinnamaldehyde		
A″	27.9	29.3		0
A′	30.2	35.2	0.155	0.109
A′	35.7	37.7	0.231	0.308
A′	44.8	46.7	0.047	0.223
A′	47.2	47.6	0.422	0.074
A″		48.7		0
A′	49.5	51.7	0.022	0.213
		p-Hydroxycinnamaldehyde		
A″	27.4	28.5		0
A′	31.0	35.6	0.435	0.047
A′	34.8	36.1	0.032	0.392
A′	37.7	47.6	0.054	0.020
A′	42.9	47.9	0.211	0.246
A″		50.1		0
A′	48.0	52.0	0.083	0.179
		3-Methoxy-4-hydroxycinnamaldehyde		
A″	27.4	31.1		0
A′	29.5	34.5	0.436	0.157
A′	33.3	35.8	0.165	0.290
A′	40.3	45.3	0.032	0.189
A′	42.2	47.0	0.262	0.052
A″		50.1		0
A′	47.6	51.1	0.121	0.232

[a] — in kK.

of the indicated $\pi \rightarrow \pi^*$ transitions have the A′ symmetry, the $n \rightarrow \pi^*$ transitions having the symmetry A″, are symmetrically forbidden. The first three calculated $\pi \rightarrow \pi^*$ transitions are bathochromically shifted in comparison with the experimental ones, which could be caused by the interaction of the solvent (ethanol) with the compounds studied.

Cinnamaldehyde

The experimental spectrum of the unsubstituted cinnamaldehyde measured in ethanol consists of three well separated $\pi \rightarrow \pi^*$ transitions at 35.1, 46.1 and 48.7 kK. The $\pi \rightarrow \pi^*$ transitions at 40.0 and 44.8 kK are present as shoulders. Besides, a very weak shoulder about 29.4 kK may be denoted as $n \rightarrow \pi^*$ transition. Our CNDO/CI calculations confirmed this assumption. The first calculated transition (Table 1) is a $n \rightarrow \pi^*$ transition with the energy of 29.0 kK. It consists mainly of the following monoexcited configurations:

$^1A''$ (29.0 kK); 49% [23 → 26], 27% [23 → 28], 20% [23 → 29].

The orbital 23 is of the n type localized mainly on O_{10} (53%), C_8 (12%) and C_9 (10%). The orbitals 26, 28, 29 are of the π^* type. While the orbitals 26 and 28 are delocalized all over the system, the orbital 29 is localised on the side conjugated chain (37% C_9, 21%.C_8, 14% O_{10}, 10% C_7).

The next three calculated transitions are of the $\pi \rightarrow \pi^*$ type and consist mainly of the following monoexcited configurations:

$^1A'$ (36.8 kK); 44% [24 → 26], 44% [25 → 27],
$^1A'$ (37.6 kK); 98% [25 → 26],
$^1A'$ (48.4 kK); 51% [24 → 26], 42% [25 → 27].

The π orbital 24 is ring localized by 25% on each C_2, C_3, C_5, and C_6, while the π orbital 25 is delocalized over the whole system. The π^* orbital 27 is ring localized by 25% on each C_2, C_3, C_5, and C_6. To the experimental transitions at 46.1 kK and 48.7 kK there correspond two calculated transitions of the $\pi \rightarrow \pi^*$ type at 49.1 kK and 52.8 kK. They arise mainly from the following monoexcited configurations:

$^1A'$ (49.1 kK); 69% [25 → 28], 27% [24 → 27],
$^1A'$ (52.8 kK); 46% [24 → 27], 31% [22→ 26], 16% [25 → 28].

The π orbital 22 is delocalized over the whole π system. Besides of the mentioned transitions, still two $\sigma \rightarrow \pi^*$ transitions (49.0 kK and 51.9 kK) exist in the calculated spectrum not observed in the experimental one.

m-Hydroxycinnamaldehyde

The experimental spectrum of m-hydroxycinnamaldehyde measured in ethanol consists of five well separated bands, corresponding to the five lowest $\pi \rightarrow \pi^*$ transitions (30.9, 35.0, 42.0, 46,9. 49.2 kK). At 27.7 kK a low intensity shoulder is present corresponding to the $n \rightarrow \pi^*$ transition. According to theoretical calculation it should be localized at 28.4 kK. It consists mainly of the following monoexcited configurations:

$^1A''$ (28.4 kK); 50% [26 → 29], 27% [26 → 31], 19% [26 → 32].

The n orbital 26 is localized mainly on O_{10} (54%), C_9 (10%), C_8 (10%). The π^* orbital 29 is delocalized over the whole molecule with an important contribution of AO's to C_7 (22%), C_8 (17%). The π^* orbital 31 is delocalized over the whole molecule, while the π^* orbital 32 is localized on C_9 (38%), C_8 (21%), O_{10} (14%), C_7 (8%).

The next four calculated transitions are of the $\pi \rightarrow \pi^*$ type, and compared with the experimental ones they have a shift of 1—4 kK towards higher energies. They consist prevailingly of the following monoexcited configurations:

$^1A'$ (35.1 kK); 38% [27 → 29], 29% [28 → 30], 18% [28 → 29],
$^1A'$ (37.6 kK); 80% [28 → 29], 10% [27 → 29],
$^1A'$ (46.7 kK); 42% [28 → 30], 40% [27 → 29],
$^1A'$ (47.6 kK); 49% [28 → 31], 42% [27 → 30].

The π orbital 27 is ring localized mainly on C_5 (32%), C_2 (20%), C_6 (18%), C_3 (16%). The π orbital 28 is delocalized with important contributions of AO's C_8, C_1, C_3, C_4. The π^* orbital 30 is ring localized by 25% on each C_2, C_3, C_5, C_6. Before the fifth short wave experimental $\pi \rightarrow \pi^*$ transition with the energy of 49.2 kK still a $\sigma \rightarrow \pi^*$ transition (48.7 kK) exists in the theoretically calculated spectrum which was not observed in the experimental one. The calculated value of the $\pi \rightarrow \pi^*$ transition (51.4 kK) was in a good agreement with the experiment. It consists mainly of the following monoexcited configurations:

$^1A'$ (51.4 kK); 38% [28 → 31], 35% [27 → 30], 20% [25 → 29].

The π orbital 25 is localized mainly on C_7 (22%), C_1 (20%), C_2 (16%), C_8 (12%) and O_{10} (10)%.

o-Hydroxycinnamaldehyde

In the experimental spectrum of o-hydroxycinnamaldehyde measured in ethanol there are

three intense bands corresponding to $\pi \rightarrow \pi^*$ transitions at 30.2 kK, 35.7 kK and 47.2 kK. The shoulders at 44.8 kK and 49.5 kK correspond to two other $\pi \rightarrow \pi^*$ transitions. A shoulder of low intensity found at 27.9 kK in the first $\pi \rightarrow \pi^*$ band may be denoted as a $n \rightarrow \pi^*$ transition. Theoretically this band was calculated at 29.3 kK and it arises of the following monoexcited transitions:

$^1A''$ (29.3 kK); 46% [26 → 29], 29% [26 → 31], 20% [26 → 32].

The n orbital 26 is localized mainly at O_{10} (54%), C_9 (12%) and C_8 (12%). The π^* orbitals 29 and 31 are delocalized over the whole π system. The π^* orbital 32 is localized mainly at C_9 (37%), C_8 (19%), O_{10} (13%), C_7 (10%).

The next four calculated transitions are of the $\pi \rightarrow \pi^*$ type and show a bathochromic shift compared with the experimental ones. They consist mainly of the following monoexcited configurations:

$^1A'$ (35.2 kK); 36% [28 → 29], 27% [28 → 30], 25% [27 → 29],
$^1A'$ (37.7 kK); 59% [28 → 29], 24% [27 → 29], 12% [28 → 30],
$^1A'$ (46.7 kK); 48% [28 → 30], 40% [27 → 29],
$^1A'$ (47.6 kK); 61% [28 → 31], 29% [27 → 30].

The π orbital 27 is ring localized at C_6 (29%), C_3 (26%), C_2 (19%), C_5 (14%). The π orbital 28 is delocalized. The π^* oribtal 30 is localized at C_5 (27%), C_6 (22%), C_3 (24%), C_2 (22%). To the last $\pi \rightarrow \pi^*$ transition found at 49.5 kK corresponds a $\pi \rightarrow \pi^*$ transition calculated at 51.7 kK. It is preceeded a $\sigma \rightarrow \pi^*$ transition, which was not observed in the experimental spectrum. This transition consists of the following monoexcited configurations:

$^1A'$ (51.7 kK); 50% [27 → 30], 27% [28 → 31].

p-Hydroxycinnamaldehyde

The experimental spectrum of p-hydroxycinnamaldehyde measured in ethanol consists of three well separated bands at 31.0, 42.9 and 48.0 kK, corresponding to $\pi \rightarrow \pi^*$ transitions. The $\pi \rightarrow \pi^*$ transitions at 34.8 kK and 37.7 kK were observed as shoulders. The low intensity $n \rightarrow \pi^*$ transition at 27.4 kK observed as a shoulder of the first $\pi \rightarrow \pi^*$ band was calculated theoretically at 28.5 kK and consists of the following monoexcited configurations:

$^1A''$ (28.5 kK); 50% [26 → 29], 26% [26 → 31], 21% [26 → 32].

The n orbital 26 is localized mainly at O_{10} (56%), C_8 (12%), C_9 (11%). The π^* orbital 29 is delocalized with an important contribution of AO's at C_7, C_8, C_9. The π^* orbital 31 is localized mainly on C_1 (22%), C_4 (18%), C_7 (16%) and C_9 (14%). The π^* orbital 32 is localized mainly on the conjugated side chain (C_9 37%, C_8 21%, O_{10} 14%).

This $n \rightarrow \pi^*$ transition in the calculated spectrum is followed by four $\pi \rightarrow \pi^*$ transitions which are bathochromically shifted against the experimentally found values. They arise mainly of the following monoexcited configurations:

$^1A'$ (35.6 kK); 53% [28 → 30], 25% [27 → 29], 12% [28 → 29],
$^1A'$ (36.1 kK); 83% [28 → 29],
$^1A'$ (47.6 kK); 66% [28 → 31], 16% [27 → 30], 10% [27 → 29],
$^1A'$ (47.9 kK); 56% [27 → 29], 26% [28 → 30], 12% [28 → 31].

The π orbital 27 is ring localized by 25% on each C_2, C_3, C_5, C_6. The π orbital 28 is delocalized with an important contribution of AO's C_8, C_4, C_1. The π^* orbital 30 is ring localized by 25% on each C_2, C_3, C_5, C_6. The fifth $\pi \rightarrow \pi^*$ transition in the experimental spectrum with the energy of 48.0 kK corresponds to the theoretically calculated transition with the energy of 52.0 kK. It is preceeded by a $\sigma \rightarrow \pi^*$ transition (50.1 kK) not observed in the experimental spectrum. This transition consists of the following monoexcited configurations:

$^1A'$ (52.0 kK); 49% [25 → 29], 37% [27 → 30], 10% [28 → 31].

The π orbital 25 is localized mainly at C_7 (25%), C_8 (20%), O_{10} (10%), C_6 (10%).

3-Methoxy-4-hydroxy cinnamaldehyde

The experimental spectrum of 3-methoxy-4-hydroxy cinnamaldehyde measured in ethanol consists of four bands corresponding to $\pi \rightarrow \pi^*$ transitions at 29.5, 40.3, 42.2, 47.6 kK. The $\pi \rightarrow \pi^*$ transition at 33.3 kK is present as a shoulder. The shoulder at 27.4 kK may be accounted to the $n \rightarrow \pi^*$ transition with the calculated value at 31.1 kK. It

consists of the following monoexcited configurations:

$^1A''$ (31.1 kK); 40% [31 → 35], 26% [31 → 37], 19% [31 → 38].

The n orbital 31 is localized mainly at O_{10} (42%), C_9 (14%), C_8 (12%). The π^* orbital 35 is localized at C_1 (14%), C_3 (10%), C_7 (25%), C_8 (17%). The π^* orbital 37 is localized at C_1 (27%), C_3 (10%), C_7 (16%), C_9 (16%) and the π^* orbital 38 is equally localized mainly at C_8 (22%), C_9 (38%), O_{10} (14%). After the $n \rightarrow \pi^*$ transition mentioned above four calculated $\pi \rightarrow \pi^*$ transitions follow which correspond to the first four $\pi \rightarrow \pi^*$ transitions of the experimental spectrum. They consist mainly of the following monoexcited configurations:

$^1A'$ (34.5 kK); 46% [34 → 35], 30% [34 → 36], 13% [33 → 35],

$^1A'$ (35.8 kK); 48% [34 → 35], 26% [33 → 35], 24% [34 → 36],

$^1A'$ (45.3 kK); 48% [33 → 35], 35% [34 → 36],

$^1A'$ (47.0 kK); 61% [34 → 37], 25% [33 → 36].

The π orbital 33 is localized at C_2 (17%), C_3 (35%), C_5 (15%), C_6 (22%). The π orbital 34 is delocalized with important contributions of AO's at C_1, C_4, C_8. The π^* orbital 36 is localized by 25% on each C_2, C_3, C_5, C_6. The theoretically calculated $\pi \rightarrow \pi^*$ transition at 51.1 kK corresponds to the experimental one at 47.6 kK. It is preceeded by a $\sigma \rightarrow \pi^*$ transition (50.1 kK) not observed in the experimental spectrum. This transition arises mainly of the following monoexcited configurations:

$^1A'$ (51.1 kK); 37% [33 → 36], 31% [32 → 35], 23% [34 → 37].

The π orbital 32 is localized mainly at C_6 (17%), C_7 (23%), C_8 (22%), O_{10} (12%).

2. Charge Density Distributions

Tables 2—6 show the calculated charge densities and dipole moments for the ground and some lower excited singlet states of the compounds investigated. Only the electron densities of the sceletal nuclei (Fig. 3) and of the hydroxyl group hydrogen are listed. The electron density of the other hydrogen atoms was changing only very little.

According to the atomic population analysis the $n \rightarrow \pi^*$ transition in the case of cinnamaldehyde is accompanied by an electronic shift from the interior of the benzene ring to the C=O group. For the hydroxy substituted cinnamaldehydes this transfer is accompanied by a remarkable charge transfer from the formyl group into the interior of the aromatic ring. For the 3-methoxy-4-hydroxy cinnamaldehyde this transition is, in contrary to the previous one, accompanied by a shift of electrons from both the OH and OCH_3 groups into the interior of the benzene ring up to the side conjugated chain.

The first long wave $\pi \rightarrow \pi^*$ transition in cinnamaldehyde is accompanied by a considerable charge transfer from the formyl group towards the interior of the benzene ring. Here the greatest change of the charge density occured on the atoms of the side conjugated chain. For both o- and m-cinnamaldehyde the first $\pi \rightarrow \pi^*$ transition is accompanied by a considerable charge transfer from the area of the aromatic ring towards the formyl group. In contrary to it, for p-hydroxycinnamaldehyde and 3-methoxy-4-hydroxy cinnamaldehyde this transition is accompanied by the shift of the charge density from the OH, OCH_3 and CHO groups towards the benzene ring.

The second $\pi \rightarrow \pi^*$ transition is accompanied in the case of cinnamaldehyde by a charge shift to the conjugated side chain. In the case of o-, m-, p-hydroxycinnamaldehyde, in the contrary, an electron shift from the CHO group towards the benzene ring take place. In the 3-methoxy-4-hydroxy cinnamaldehyde this transition is accompanied by an electron shift from both the OCH_3 and OH groups towards the side conjugated chain.

The third $\pi \rightarrow \pi^*$ transtition in cinnamaldehyde is accompanied by an electron shift from the conjugated chain to the benzene ring. A similar charge shift occured in the case of o-, m-hydroxycinnamaldehydes and 3-methoxy-4-hydroxy cinnamaldehyde. For p-hydroxycinnamaldehyde this transition is accompanied by a charge transfer from the OH group trough the benzene ring to the C=O group.

The fourth and fifth $\pi \rightarrow \pi^*$ transitions in the compounds investigated are accompanied by a variable charge change on every heavy atom (Tables 2—6).

Summary

The CNDO/CI method has been used for the theoretical investigation of the electronic spectra of cinnamaldehyde and its OH and OCH_3 derivatives.

Table 2. Calculated Charge Densities and Dipole Moments for the Ground and some Lower Singlet Excited States of Cinnamaldehyde.

ν, kK	C_1	C_2	C_3	C_4	C_5	C_6	C_7	C_8	C_9	O_{10}	$\mu \times 10^{29}$, C.m
0	−.015	−.030	−.021	0.05	−.014	−.029	.059	−.093	.251	−.425	1.40
29.0	−.147	.207	.132	−.083	.155	.195	−.175	−.265	.168	−.503	4.66
36.8	−.164	−.013	−.108	−.030	−.084	−.011	−.253	−.166	.258	.066	2.76
37.6	−.119	.222	.129	−.018	.148	.209	−.291	−.217	.105	−.516	5.50
48.4	.141	−.222	−.167	.190	−.179	−.207	.082	.116	.220	−.375	1.16
49.1	−.053	.018	−.052	.063	−.005	−.004	−.141	−.185	.144	−.395	3.10
52.8	−.058	.024	−.002	.074	−.050	.023	−.133	−.226	.178	−.398	2.89

Table 3. Calculated Charge Densities and Dipole Moments for the Ground and some Lower Singlet Excited States of m-Hydroxycinnamaldehyde.

ν, kK	C_1	C_2	C_3	C_4	C_5	C_6	C_7	C_8	C_9	O_{10}	O_{11}	H_{12}	$\mu \times 10^{29}$, C.m
0	−.035	−.031	−.029	.011	−.021	.125	.022	.047	.237	−.416	−.329	.220	2.07
28.4	−.163	−.010	−.073	−.067	−.032	.147	−.171	−.123	.259	−.056	−.315	.221	2.23
35.1	−.180	.175	.080	−.082	.268	.341	−.283	−.227	.098	−.513	−.234	.223	5.90
37.6	−.114	−.051	−.051	−.026	−.119	.154	−.260	−.075	.218	.001	−.309	.222	2.40
46.7	.119	−.265	−.103	.134	−.157	−.016	.061	.149	.205	−.372	−.302	.223	1.68
47.6	−.055	−.063	.109	−.013	−.001	.095	−.102	.194	.079	−.450	−.308	.220	2.90
51.4	−.195	−.006	.055	−.104	.239	.153	−.112	−.035	.018	−.368	−.254	.226	2.86

Table 4. Calculated Charge Densities and Dipole Moments for the Ground and some Lower Singlet Excited States of o-Hydroxycinnamaldehyde.

ν, kK	C_1	C_2	C_3	C_4	C_5	C_6	C_7	C_8	C_9	O_{10}	O_{11}	H_{12}	$\mu \times 10^{29}$, C.m
0	.005	−.057	−.001	−.020	.156	−.062	.071	−.104	.248	−.424	−.323	.219	1.90
29.3	−.139	.009	−.009	−.094	.144	.026	−.118	−.182	.252	−.161	−.310	.219	0.69
35.2	−.196	.200	.194	−.123	.258	.288	−.238	−.241	.109	−.516	−.257	.219	5.90
37.7	−.165	−.011	−.132	−.037	.135	−.074	−.218	−.073	.236	.022	−.304	.219	2.28
46.7	.101	−.188	−.160	.135	.008	−.224	.105	.154	.207	−.374	−.292	.219	0.98
47.6	−.021	−.108	−.029	.027	.194	−.149	.024	.096	.126	−.423	−.298	.220	1.62
51.7	−.109	.047	−.017	.043	.190	.003	−.129	−.280	.086	−.350	−.284	.220	3.80

Table 5. Calculated Charge Densities and Dipole Moments for the Ground and some Singlet Excited States of p-Hydroxycinnamaldehyde.

ν, kK	C_1	C_2	C_3	C_4	C_5	C_6	C_7	C_8	C_9	O_{10}	O_{11}	H_{12}	$\mu \times 10^{29}$, C.m
0	.134	−.037	−.028	.012	−.026	−.025	.008	−.045	.234	−.421	−.281	.183	1.68
28.5	.036	−.066	−.125	−.017	−.112	−.050	−.165	−.064	.272	.002	−.285	.183	3.50
35.6	.524	−.490	−.473	.496	−.411	−.392	.055	.507	.193	−.271	−.162	.185	3.80
36.1	−.068	−.004	−.184	−.057	−.158	.006	−.410	−.101	.292	.325	−.285	.186	5.53
47.6	−.108	.488	.242	−.062	.273	.478	−.593	−.345	.001	−.579	−.276	.183	8.87
47.9	−.098	−.107	.160	.020	.140	−.104	−.313	.813	−.326	−.509	−.164	.184	3.03
52.0	.082	.005	−.076	.041	−.075	.008	−.256	−.131	.175	−.237	−.263	.188	1.70

Table 6. Calculated Charge Densities and Dipole Moments for the Ground and some Lower Singlet Excited States of 3-Methoxy-4-hydroxycinnamaldehyde.

ν. kK	C_1	C_2	C_3	C_4	C_5	C_6	C_7
0	.147	.123	−.056	−.001	−.019	−.049	.070
31.1	.176	.139	−.044	.045	−.043	−.066	−.029
34.5	.626	−.188	−.579	.456	−.342	−.589	.037
35.8	−.087	.467	.355	−.114	.099	.245	−.441
45.3	−.063	.169	−.338	−.038	−.115	−.069	−.488
47.0	.100	.151	−.043	−.037	.309	−.123	−.350
51.1	.092	.256	.021	.013	−.007	.011	−.182

C_8	C_9	O_{10}	O_{11}	H_{12}	O_{13}	C_{14}	$\mu \times 10^{29}$, C.m
−.113	.274	−.442	−.288	.188	−.269	.023	1.60
−.094	.232	−.450	−.267	.188	−.227	.024	2.26
.315	.236	−.313	−.141	.129	−.203	.031	3.26
−.408	.087	−.559	−.286	.190	−.108	.036	7.53
−.178	.334	.434	−.277	.188	−.243	.022	7.13
.567	−.321	−.592	−.132	.188	−.161	.026	5.47
−.252	.154	−.462	−.260	.186	−.181	.047	4.23

The calculated values of the transition energies were found in a good agreement with the experimental ones. The transitions with the energies of 27—29 kK in the experimental spectra of the compounds investigated correspond to the $n \rightarrow \pi^*$ transitions in the theoretical spectra and are responsible for the colour of these substances.

The OH and/or OCH_3 substitution of the aromatic ring caused a bathochromic shift of both the calculated and experimental $\pi \rightarrow \pi^*$ transitions. The values of the calculated transition energies and the electron distribution depend, however, on the parametrization which is assumed. We have used the parametrization of Kuehnlenz and Jaffé [10] which was recently successfully applied on a larger scale for calculations of electronic spectra of organic molecules.

[1] M. Remko and J. Polčin, Chem. Zvesti **31**, 171 [1977].
[2] M. Remko and J. Polčin, Monats. Chem. in press.
[3] J. Del Bene and H. H. Jaffé, J. Chem. Phys. **48**, 1807 [1968].
[4] K. V. Sarkanen and C. H. Ludwig, Lignins, Wiley Intersci., New York 1971.
[5] J. Polčin and W. H. Rapson, Pulp Pap. Mag. Canada **70**, T555 [1969]; **72**, T103 [1972]; **72**, T115 [1972].
[6] J. Polčin, Zellstoff und Papier **22**, 226 [1973].
[7] J. Polčin, Papier a Celuloza **29**, V69 [1974].
[8] A. Krutosikova, J. Sura, S. Stankovsky, J. Polčin, and J. Kovac, Cellulose Chem. Technol. **9**, 51 [1975].
[9] N. Mataga and K. Nishimoto, Z. Phys. Chem., Frankfurt **13**, 140 [1957].
[10] G. Kuehnlenz and H. H. Jaffé, J. Chem. Phys. **58**, 2238 [1973].
[11] L. E. Sutton, Tables of Interatomic Distances and Configuration in Molecules and Ions. Spec. Publ. N. 11 and 18 The Chemical Society London 1958 and 1965.